according to the manufacturers' instructions. RNA concentration was determined by the measurement of UV absorbance spectra, and the total RNA profile was analyzed using an Agilent 2100 Bioanalyzer (Agilent Technologies Japan, Tokyo, Japan) to determine RNA integrity number (RIN). Expression profiles of the RNA samples with an RIN $\geqq$6.9 were determined using Affymetrix Human or Mouse Gene 1.0ST arrays (Affymetrix Japan, Tokyo, Japan) according to the manufacturer's instructions. The Ambion WT Expression Kit (Life Technologies Japan, Tokyo, Japan) and the GeneChip WT Terminal Labeling and Controls Kit (Affymetrix Japan) were used to generate amplified and biotinylated sense-strand DNA targets from expressed transcripts (100 ng of total RNA). Manufacturer's instructions were followed for hybridization, washing, and scanning steps, and CEL files were generated. CEL files were imported into Partek Genomics Suite software (Partek, St Louis, MO, USA), and both exon-level and gene-level estimates were obtained for all transcript clusters. The gene-level estimates were subjected to statistical analysis and hierarchical and partitioning clustering by the software. Transcript clusters with differential expression were investigated for functional inter-relatedness and networks using the Ingenuity Pathway Analysis (IPA) program (Ingenuity Systems, Redwood, CA, USA).

Reverse-Transcription and Quantitative Polymerase Chain Reaction

To validate the microarray data, we performed quantitative real-time reverse-transcription polymerase chain reaction (RT-PCR) on individual genes. We selected 17 genes of interest as potential targets for real-time RT-PCR; the corresponding gene-specific primer pairs are listed in Supplementary Table S1. Three genes, *RN18S1*, *ACTB*, and *GAPDH*, were used as internal controls. Each sample was reverse-transcribed to first-strand cDNA using 1 μg of total RNA, random primers and the High-Capacity cDNA Reverse-Transcription Kit (Life Technologies Japan). For each quantitative PCR reaction, 0.5% of the total complementary DNA yield was used. Transcript quantifications were carried out on a Thermal Cycler Dice® Real-Time System Single (Takara, Kyoto, Japan). Each reaction was performed using the appropriate amount of complementary DNA, optimized amounts of forward and reverse primers, and 12.5 mL of 2 × SYBR Green Ready Reaction Mix with Rox (Life Technologies Japan) in a total volume of 25 mL. Dissociation curves were generated for all wells. No primer dimers were observed.

Tissue Processing and Immunofluorescence Microscopy

Animals deeply anesthetized with pentobarbital were perfused intracardially with saline followed by cold 4% paraformaldehyde (PFA) in PBS. The brains were removed, immersed for 12 h in the same 4% PFA fixative, then in 20% followed by 30% sucrose in PBS for 24 h at 4 °C. The brains were stored as paraffin-embedded blocks. Tissue sections (4-μm thick) were cut from the blocks on a microtome and mounted from warm water (42 °C) onto slides. Sections were allowed to dry overnight at room temperature, deparaffinized in xylene, and rehydrated through a graded ethanol series. Antigen retrieval was performed by boiling sections in plastic Coplin jars containing sodium citrate buffer (10 mM citric acid, 0.05% Tween 20, pH 6.0) using a water bath (100 °C) for 10 min followed by cooling for 30 min to room temperature. Sections were blocked with a solution containing 1 × Block Ace (Dainippon Pharmaceutical, Osaka, Japan) for 30 min at room temperature, incubated with anti-PCSK1 (sc-100578, 1:50, Santa Cruz Biotechnology, Santa Cruz, CA, USA) and antineuron-specific nuclear protein (NeuN) (ABN78, 1:1000, Merck Japan, Tokyo, Japan) antibodies in 10% Block Ace at 4 °C overnight, and then incubated with an Alexa Fluor-labeled second antibody (Invitrogen Japan, Tokyo, Japan) for 45 min at room temperature. Confocal images were acquired using an LSM510 META Confocal Microscope System (Carl Zeiss MicroImaging, Tokyo, Japan).

Western Blot Analysis

Frozen hippocampus samples were homogenized in buffer containing 150 mM NaCl, 1.0% NP-40, 0.5% sodium deoxycholate, 0.1% sodium dodecyl sulfate (SDS), 50 mM Tris-HCl, pH 8.0) with 2% protease inhibitor, and a 5% phosphatase inhibitor cocktail (Nacalai Tesque, Kyoto, Japan) using a tissue homogenizer at 1500 rpm for 30 s. The homogenates were mixed with 2 × SDS sample buffer and subjected to 10% SDS polyacrylamide gel electrophoresis followed by western blotting using anti-PCSK1 (sc-100578), anti-PCSK2 (MAB6018, R&D Systems, Minneapolis, MN, USA), and anti-GAPDH (14C10, Cell Signaling Technology, Beverly, MA, USA) antibodies with appropriate fluorophore-conjugated secondary antibodies (LI-COR, Lincoln, NE, USA). Quantitative detection of fluorescent bands was performed using the Odyssey infrared imaging system (LI-COR). The blots were stained with Ponceau S (Sigma-Aldrich Japan, Tokyo, Japan), and digital images generated by a document scanner were used to quantitate total proteins on the blots in Image Gauge software (Fujifilm, Tokyo, Japan).

Statistical Analysis

Gene-level estimates from human microarray data were subjected to 3-way analysis of variance (ANOVA); then, the results of a specific comparison (AD vs. non-AD) were obtained using false discovery rate (FDR, $q < 0.05$) controlling procedures (Benjamini and Hochberg 1995). Gene-level estimates from mouse microarray data were subjected to ANOVA, and the obtained list of transcript clusters with $P < 0.05$ was subjected to a specific comparison (3x-TG-AD-H vs. non-Tg) with FDR ($q < 0.05$) control and a fold-change >1.3 as a threshold for the comparison. Statistical analysis of western blot data was performed by unpaired *t*-test using JMP 8.0 software (SAS Institute, Raleigh, NC, USA). A *P*-value <0.05 was considered statistically significant.

Results

Clinical and Pathological Features of Subjects

High-quality RNA samples with an RIN $\geqq$6.9 from the gray matter of frontal and temporal cortices and hippocampi of 88 postmortem brains were subjected to microarray analysis. Among these, 26 subjects were pathologically diagnosed as having AD or an AD-like disorder. Only those results that

Table 1
Mean *F* ratios in 3-way ANOVAs of the microarray data

Comparison	Mean *F* ratios								
	Frontal cortex			Temporal cortex			Hippocampus		
	A	B	C	A	B	C	A	B	C
AD vs. non-AD	1.77	3.97	5.28	2.15	5.85	10.24	3.50	22.14	23.49
VD vs. non-VD	0.83	0.64	0.66	1.06	1.01	0.98	1.37	2.37	2.49
Sex	2.30	1.91	2.91	2.57	1.33	1.27	2.73	3.33	2.71

Note: A: mean *F* ratios for all transcript clusters (33 297) are shown. *B*: mean F ratios for transcript clusters (1387) exhibiting significantly altered expression between AD and non-AD hippocampal RNAs. *C*: mean F ratios for the top 200 transcription clusters in *B*. Statistical power analysis revealed that the smallest sample size that could be set for the 3-way ANOVAs was 5 with a significance (*P*-value) level of 0.01 and power of 0.8.

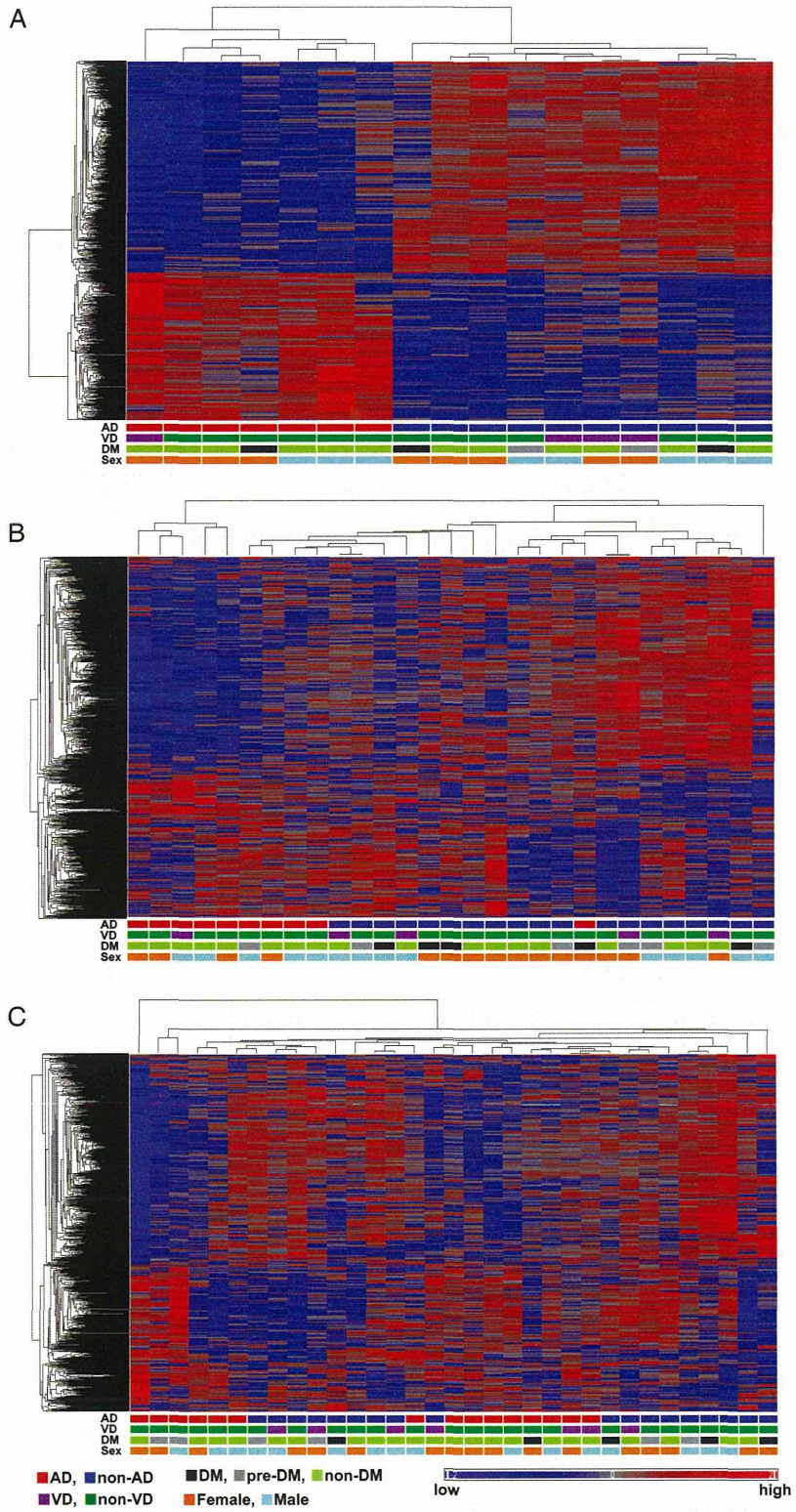

Figure 1. Hierarchical and partitioning clustering of the 1387 transcript clusters in the 3 regions of brain. (*A*) Cluster heat map of the 1387 transcript clusters based on expression data in the hippocampus. (*B*) Cluster heat map of the 1387 transcript clusters based on expression data in the temporal cortex. (*C*) Cluster heat map of the 1387 transcript clusters based on expression data in the frontal cortex. AD (red), non-AD (nAD, dark blue); vascular dementia (VD, dark green), non-VD (nVD, purple); diabetes mellitus (DM, black), prediabetes (pre-DM, gray), non-DM (light green); female (F, orange), male (M, light blue), In the heat map, blue represents a lower expression level and red indicates a higher expression level.

passed examinations for quality assurance and quality control of the GeneChip Human Gene 1.0 ST arrays were retrieved. In total, we obtained gene expression profiles from the following samples: 33 frontal cortex samples, among which 15 were from AD patients; 29 temporal cortex samples, among which 10 were from AD patients; 17 hippocampus samples, among

which 7 were from AD patients (see Supplementary Tables S2 and S3). NPs, assessed according to the CERAD guidelines (Mirra et al. 1991), were frequent (score of 3) in all 16 AD brains that provided RNA samples of suitable quality. The distribution patterns of neurofibrillary tangles (NFTs), assessed according to Braak stage (Braak and Braak 1991), were all stage V–VI. Two subjects given a pathological diagnosis of AD had been clinically diagnosed as having vascular dementia (VD), while another 3 subjects with a pathological diagnosis of AD had been clinically diagnosed with DM or prediabetes (defined as a blood glucose level of 140–199 mg/dL 2 h after a 75-g oral glucose tolerance test, or a blood glucose level of 110–125 mg/dL in the fasting condition) (see Supplementary Tables S2 and S3).

Altered Gene Expression Profiles in the Hippocampus, Temporal Cortex, and Frontal Cortex with AD Pathology

Three-way ANOVA of the microarray data with AD versus non-AD, VD versus non-VD, and female versus male as factors revealed that the comparison of AD versus non-AD exhibited the highest mean *F* ratio (3.50) based on expression data for all 33 297 transcript clusters obtained from hippocampal RNAs (Table 1). In total, 348 transcript clusters in the temporal cortex (98 up and 250 down) and 1387 transcript clusters in the hippocampus (569 up and 818 down), but none in the frontal cortex, showed significantly altered expression levels in AD versus non-AD brains (see Supplementary Tables S4 and S5). Of the 348 transcript clusters in the temporal cortex, 125 were also among the 1387 transcript clusters in the hippocampus. The mean *F* ratios for the 1387 transcript clusters identified in the hippocampus (Table 1) confirmed that the gene expression profile in the hippocampus is the most significantly altered in AD brain. No genes in any cluster showed a significant difference in expression levels between patients with DM or prediabetes (data not shown).

Hierarchical and partitioning clustering of the 1387 hippocampal transcript clusters (Fig. 1*A*) based on data from hippocampal samples revealed clustering of the 7 AD cases separately from the 10 non-AD cases, with statistical significance. Using data from temporal cortex samples, 9 of 10 AD cases were clustered together (Fig. 1*B*). Using data from frontal cortex samples, 6 and 8 AD cases were separately clustered out of 15 AD cases, and 8 and 9 non-AD cases were separately clustered out of 18 non-AD cases (Fig. 1*C*). Thus, the expression profiles of the 1387 transcript clusters identified as being altered in the hippocampus are similarly changed in the temporal and frontal cortices, but to lesser extents.

Genes Whose Expression Levels are Significantly Altered in AD Hippocampus

To retrieve genes whose expression levels were significantly altered in AD brains in comparison with non-AD brains, it is essential to consider the changes in the population of brain cells in AD brains. Therefore, we compared the expression levels of genes encoding specific markers for 4 major types of brain cells, namely, neurons, astrocytes, oligodendrocytes, and microglia (Table 2). The expression levels of 10 neuronal markers, including *RBFOX3* encoding NeuN (Dredge and Jensen 2011), which is expressed in about 68% of cells in the gray matter of the adult cerebral cortex (Azevedo et al. 2009), were consistently decreased in AD brains relative to the levels in non-AD brains, most significantly in the hippocampus. Conversely, the expression levels of *GFAP*, *S100B*, and *AQP4* transcripts, representing the astrocyte population, and to a lesser extent those for *AIF1*, *LGALS3*, *CD68*, and *EMR1* representing the microglial population, were increased, especially in the temporal cortex and hippocampus. The expression levels of *MBP*, *SOX10*, *MOG*, and *MAG*, representing the oligodendrocyte population, were largely unchanged. These data are likely to reflect neuronal loss and gliosis in AD brains; neuronal loss is most evident in the hippocampus, and gliosis is most evident in the temporal cortex and hippocampus.

Taking the mean relative expression levels of these markers in different brain regions (Table 2) into account, we selected the top 200 transcript clusters that exhibited a fold-change >1.563 from among the 1387 transcript clusters identified as being altered in the hippocampus (see Supplementary Table S6). In AD brains, 143 of the 200 transcript clusters were markedly downregulated in the hippocampus beyond the level expected based on the cell population change. Because of the population change in AD brains, the number of upregulated genes in AD brains was likely to have been underestimated (57 transcript clusters in see Supplementary Table S6).

We next individually analyzed the raw expression levels of 12 genes showing significant alterations (downregulated: *MET*, *PCSK1*, *RGS4*, *HS3ST2*, *NPTX2*, *NEUROD6*, *RAB27B*, *HCN1*, *HOMER1*; upregulated: *GJA1*, *AEBP1*, *GALNTL2*) in 3 brain regions from each subject (see Supplementary Fig. 1, left panels), confirming that AD hippocampi exhibited the most significant alterations of gene expression (Fig. 2*A*). The expression levels of individual exons within the 12 genes were also most significantly altered in the hippocampi of AD

Table 2
Altered expression levels of marker genes for various brain cell types in AD brains

Cell type	Relative expression (% non-AD)			
	Marker gene	Frontal cortex	Temporal cortex	Hippocampus
Astrocytes	*GFAP*	126.95	162.93	136.25
	S100B	101.32	128.95	125.96
	AQP4	107.40	132.57	146.39
	Mean	111.89	141.48	136.20
	SD	13.39	18.66	10.22
Oligodendrocytes	*MBP*	101.57	102.15	96.83
	SOX10	98.41	100.62	103.07
	MOG	104.55	130.64	116.20
	MAG	108.60	116.36	102.50
	Mean	103.28	112.44	104.65
	SD	4.34	14.05	8.20
Microglia	*CD68*	103.66	134.19	110.55
	AIF1	96.81	114.67	107.54
	LGALS3	103.20	114.04	112.30
	EMR1	101.13	115.21	102.74
	Mean	101.20	119.53	108.28
	SD	3.12	9.78	4.19
Neurons	*RBFOX3*	84.26	79.43	63.82
	ENO2	98.75	94.25	78.10
	CHGA	94.11	89.88	53.31
	TUBB	96.40	96.03	86.51
	SYP	92.00	86.73	65.49
	NEFH	90.60	96.27	54.13
	NEFM	97.17	90.80	64.43
	NEFL	89.76	83.80	58.93
	SNAP25	86.35	79.55	60.83
	SYT1	87.70	82.85	63.15
	Mean	91.71	87.96	64.87
	SD	4.86	6.45	10.27

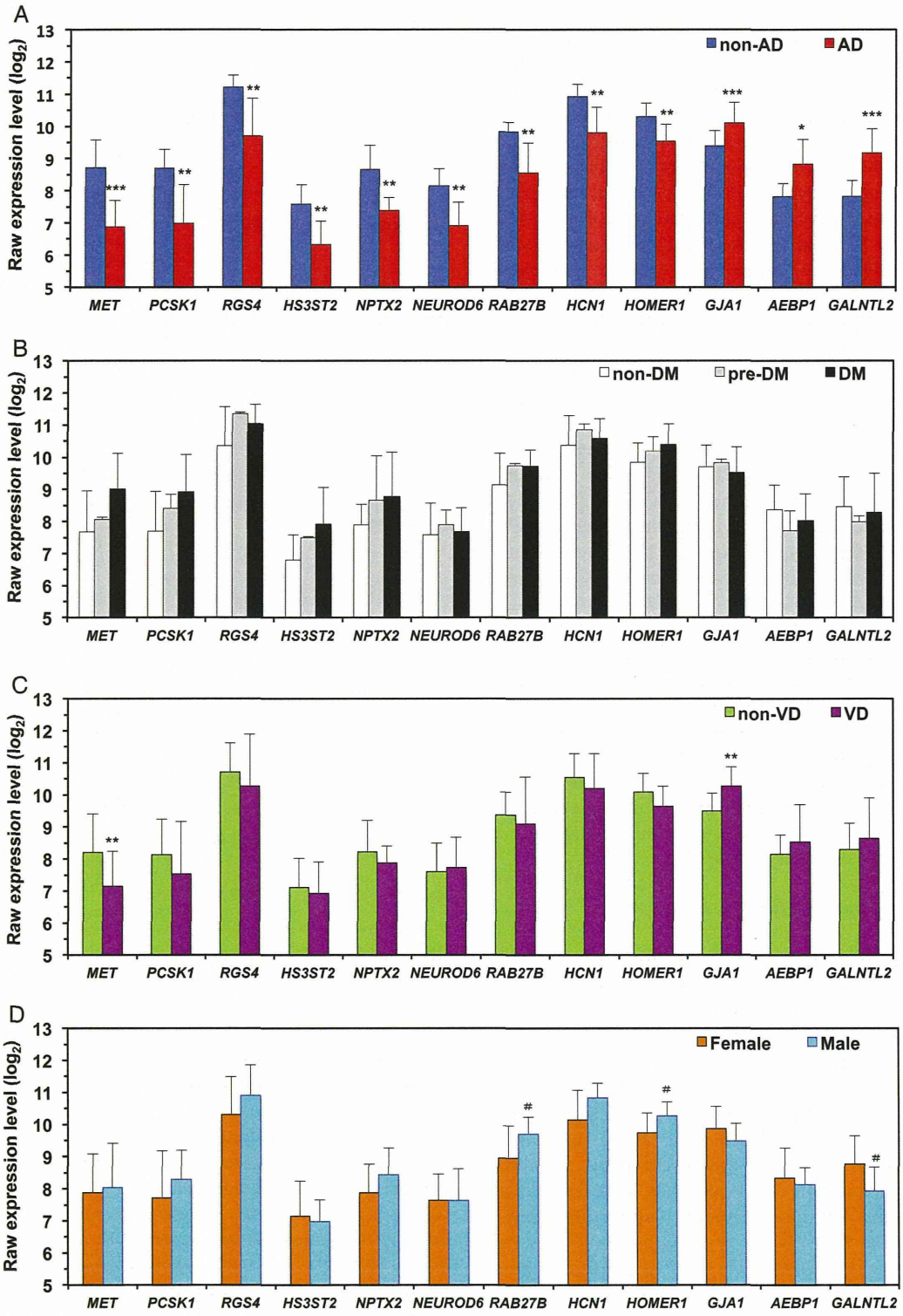

Figure 2. Comparison of the raw expression levels of 12 genes whose expression was significantly altered in the AD hippocampus. (*A*) Comparison between non-AD and AD cases. Dark blue box, non-AD ($N = 10$); red box, AD ($N = 7$). (*B*) Comparison between non-DM and pre-DM/DM cases. Open box, non-DM ($N = 12$); gray box, prediabetes (pre-DM, $N = 2$); black box, DM ($N = 3$). (*C*) Comparison between non-VD and VD cases. Green box, non-VD ($N = 13$); purple box, VD ($N = 4$). (*D*) Comparison between female and male cases. Orange box, female ($N = 9$); light blue box, male ($N = 8$). Four-way ANOVA was performed with the list of 1387 transcript clusters altered in the hippocampus, and the *P*-value for each comparison was determined by Fisher's Least Significant Difference method. Log_2 transformed mean values with SD for the raw expression levels of 12 genes are shown in each bar graph. $^{\#}P < 0.05$, $^{*}P < 0.01$, $^{**}P < 0.005$, $^{***}P < 0.001$. In *B*, non-DM ($N = 12$) and pre-DM + DM ($N = 5$) were compared; none of the 12 altered genes showed a significant difference.

brains, being altered to a lesser extent in the temporal cortex and much less so in the frontal cortex, in accordance with the pathological severity (see Supplementary Fig. 1, right panels). None of the 12 genes examined exhibited a significant alteration between non-DM and prediabetes/DM cases (Fig. 2*B*). The genes that were downregulated in AD hippocampus

exhibited slightly increased expression in subjects with prediabetes or DM, but this increase was not statistically significant. Among the 12 genes with altered expression, a few genes (*MET* and *GJA1* for VD; *RAB27B*, *HOMER1* and *GALNTL2* for sex) exhibited moderate but statistically significant alterations between non-VD and VD or between sexes (Fig. 2*C,D*).

Among the top 200 transcription clusters, 147 genes were Functions/Pathways eligible genes in the computational gene network prediction tool IPA. These were categorized as genes significantly relevant to genetic disorders [105], neurological diseases [85], gastrointestinal diseases [74], and others. Genes categorized into genetic disorders were subcategorized as genes significantly relevant to schizophrenia [29], bipolar disorder [26], coronary artery disease [25], Crohn's disease [23], noninsulin-dependent DM [23], amyotrophic lateral sclerosis [22], Huntington's disease [22], AD [21], Parkinson's disease [14], obesity [12], and others (Table 3).

Among the top 200 transcription clusters, 145 genes were eligible for generating IPA networks. The most relevant network included downregulated genes such as *MET*, *PCSK1*, *PTPN3*, *SERPINF1*, and *VEGFA*, and upregulated genes such as *AEBP1* and *TXNIP* (Fig. 3*A*; Network 1). The second-most relevant network consisted of the genes encoding GABA receptors (*GABRA1*, *GABRA4*, *GABRA5*, *GABRG2*), synaptotagmin members, syntaxin, potassium channels, and regulators of G protein signaling. Expression of all of these genes was markedly decreased in the AD hippocampus (Fig. 3*B*; Network 2), reflecting the neuronal dysfunction in AD brain. The third-most relevant network consisted of genes regulated by insulin signaling pathways, as discussed below (Fig. 3*C*; Network 3). The alterations in the expression levels of the genes constituting these 3 networks were well preserved in the temporal cortex and to a lesser extent in the frontal cortex of AD brains (see Supplementary Table S6).

Altered Gene Expression Profiles in Mouse AD Hippocampus

We next performed microarray analysis of hippocampal RNA prepared from 14-month-old 3xTg-AD hemizygous (3x-Tg-AD-h; $N=3$) and homozygous (3xTg-AD-H; $N=3$) male mice for APP_{Swe} and $MAPT_{P301L}$ transgenes with a homozygous $PS1_{M146V}$ mutation and non-Tg mice ($N=3$). The transgenic mice exhibited severe learning and memory deficits with progressive development of amyloid plaques and NFTs as previously described (Oddo et al. 2003). We compared the expression levels of genes encoding specific markers for the 4 major types of brain cells, and found no differences among the 4 groups (Table 4), supporting a previous observation that there is no obvious neuronal loss in 3xTg-AD mice (Oddo et al. 2003). Then, 2713 transcript clusters showing a significant difference among the 3 groups (ANOVA, $P<0.05$) were further compared between samples from non-Tg mice and each line of 3xTg-AD mice with FDR control ($q<0.05$). As a result, 406 clusters from 3xTg-AD-H samples and 243 clusters from 3xTg-AD-h samples were found to have a fold-change >1.3 compared with non-Tg samples (see Supplementary Table S7). Ninety-three transcript clusters were shared between these groups. Hierarchical clustering of the 406 transcript clusters identified as having changed in 3xTg-AD-H samples was performed among the 3 groups, revealing that the expression profiles in 3xTg-AD-H samples were significantly different from those in non-Tg samples, and that the differences were partly shared by 3xTg-AD-h samples (Fig. 4*A*).

Table 3
Genes significantly enriched in genetic disorders among those whose expression was significantly altered in AD hippocampus

Diseases and disorders	*P*-value*	Genes**
Schizophrenia	6.77E-14	*APBA2, ATP2B2, CHRNB2, CPLX1, EGF, EGR3, ELAVL4, GABRA1, GABRA4, GABRA5, GABRG2, GLRB, HOMER1, HPRT1, LARGE, NEFL, PCSK1, PPP1R16B, PRKCB, RGS4, RGS7, RIT2, SLC17A7, SLC7A11, SNAP25, STMN2, SYT4, SYT7, TXNIP*
Bipolar disorder	6.08E-06	*ARL15, ATP2B2, CA5B, CHRNB2, CNGA3, DUSP6, FABP3, FAM19A1, GABBR2, GABRA1, GABRA4, GABRA5, GABRG2, GALNTL2, KCNJ6, LDB2, MAN1A1, NDFIP2, NEFL, PHACTR1, PRKCB, PTPRN2, RGS4, RIT2, SYN1, WDR49*
Coronary artery disease	1.04E-04	*ARL15, ATRNL1, FAM19A1, GABRA1, GABRA4, GABRA5, GABRG2, GFRA2, HS3ST2, HS6ST3, IFLTD1, KCNK9, LAMA4, LARGE, LDB2, MAPK9, NEDD4L, NPTXR, PHACTR1, PTPRN2, RIT2, SEL1L3, SNTB1, VEGFA, WBSCR17*
Crohn's disease	2.46E-04	*APBA2, ATP2B2, ATRNL1, DLGAP1, FAM19A1, GABRA4, GLRB, HCN1, HOPX, HPRT1, HS6ST3, IL12RB2, LDB2, MAN1A1, NEDD4L, PTPRN2, QPCT, RGS7, RIMBP2, RIT2, SEL1L3, SNAP25, SYT7*
Noninsulin-dependent diabetes mellitus	4.15E-03	*AACS, ANO3, ARL15, CA5B, CHRNB2, COL21A1, GDAP1L1, HS3ST2, HS6ST3, KCNJ6, LARGE, LDB2, NPTXR, PCSK1, PRKCB, RAB27B, RGS7, RIT2, SNTB1, TSPAN5, VEGFA, WBSCR17, YWHAG*
Amyotrophic lateral sclerosis	2.30E-08	*ATP2B2, ATP2B3, FAM19A1, FRMPD4, GABBR2, GABRA1, GABRA4, GABRA5, GABRG2, GALNTL2, INA, LARGE, NEFH, NEFL, NPTXR, PFKP, PPP1R16B, PTPRN2, RIMBP2, SYN1, VCAN, WBSCR17*
Huntington's disease	2.79E-07	*AEBP1, ATP2B2, CCKBR, GABRA1, GABRA4, GABRA5, GABRG2, GJA1, GLRB, GNG3, HOMER1, HPCA, MAN1A1, NEFL, OXR1, PRKCB, PTPN3, PTPN5, RGS4, SLC17A7, SNAP25, VCAN*
Alzheimer's disease	1.77E-04	*ANO3, ATP6V1G2, ATRNL1, CHRNB2, EGF, FAM19A1, FRMPD4, GABBR2, GABRA1, GABRA4, GABRA5, GABRG2, HOMER1, LARGE, MAPK9, NEFH, NEFL, PREP, PRKCB, SLC6A7, WBSCR17*
Parkinson's disease	2.21E-03	*ATRNL1, CA5B, CHRNB2, FRMPD4, GABBR2, GABRA1, GABRA4, GABRA5, GABRG2, HOMER1, KCNJ6, SH3RF1, SNAP25, SYN1*
Obesity	1.54E-04	*AEBP1, CA5B, CCKBR, CHRNB2, CPT1C, GABRA1, GABRA4, GABRA5, GABRG2, PCSK1, SYT4, VEGFA*

Note: Diseases and disorders in which more than 10 genes are enriched are listed.
*P-value by Fisher's exact test. **Upregulated genes are shown with underline.

Among the 406 mouse transcription clusters, 109 genes were Functions/Pathways eligible genes in IPA. These were categorized as genes significantly relevant to genetic disorders [62], neurological disease [43], gastrointestinal disorders [35], and others. Genes categorized into genetic disorders were subcategorized as genes significantly relevant to bipolar disorder [20], noninsulin-dependent DM [17], coronary artery disease [16], AD [13], Parkinson's disease [9], obesity [7], and others (Table 5). These categories and subcategories were essentially the same as those detected as relevant in the AD hippocampus. Among the 406 transcription clusters, only 120 genes were eligible for generating IPA networks, and the most relevant network included 11 genes that were downregulated and 5 that were upregulated in the hippocampi of 3xTg-AD-H mice (Fig. 4*B*). The raw expression level of *Pcsk1* was most significantly decreased in the hippocampi of 3xTg-AD-H mice and to a lesser extent in those of 3xTg-AD-h mice in comparison with non-Tg mice, while that of *Ide* was significantly increased in the hippocampi of both 3xTg-AD-H and 3xTg-AD-h mice (Fig. 4*C*).

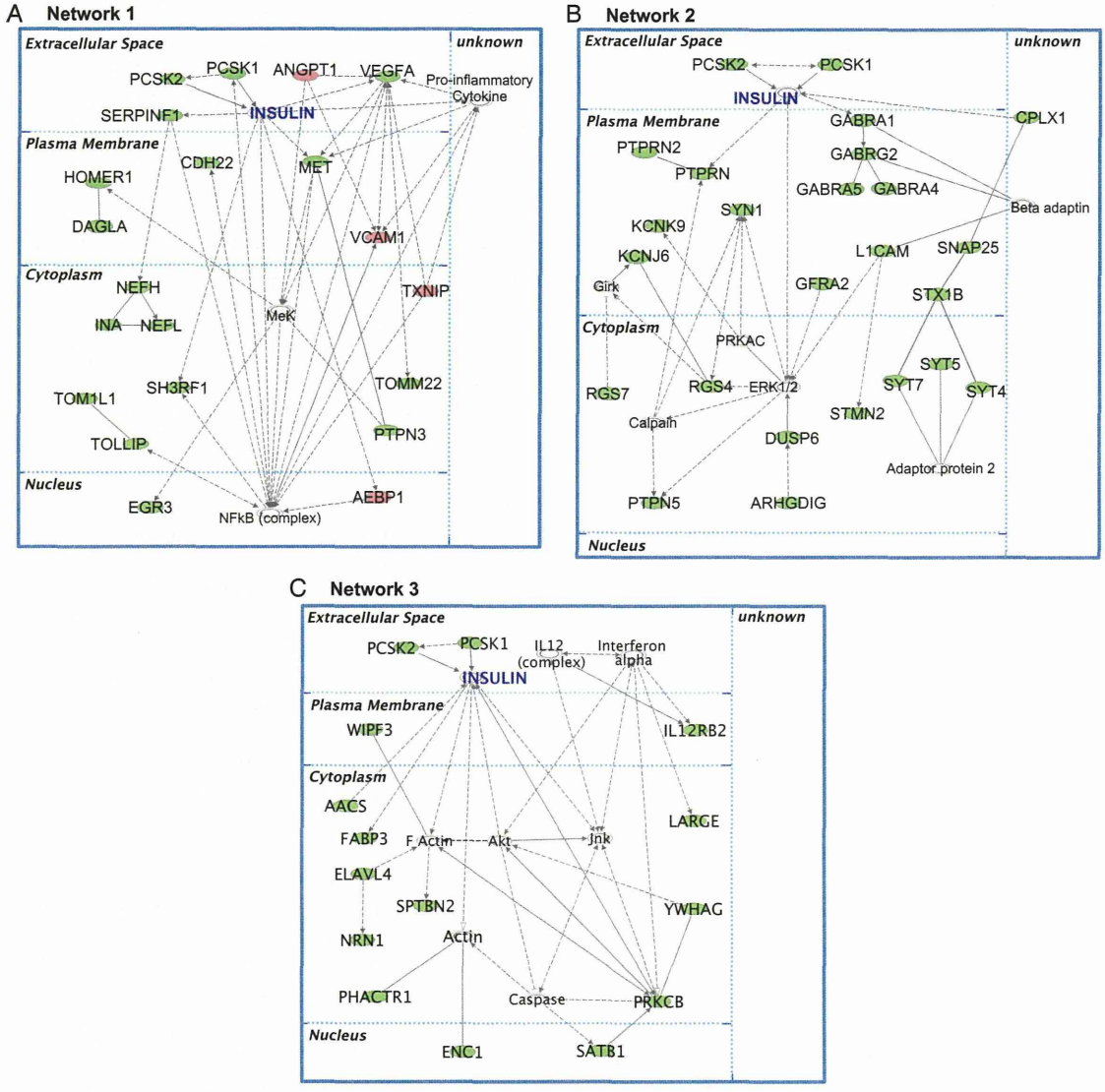

Figure 3. Top 3 networks of genes whose expression was significantly altered in the AD hippocampus. Among the top 200 transcription clusters shown in Supplementary Table S6, 145 genes were eligible for generating networks excluding microRNA–mRNA interactions by IPA. (*A*) Network 1 includes 16 downregulated genes (*MET, PCSK1, PTPN3, SERPINF1, VEGFA, NEFH, EGR3, HOMER1, INA, DAGLA, CDH22, NEFL, TOM1L1, TOLLIP, SH3RF1, TOMM22*), and 4 upregulated genes (*AEBP1, TXNIP, VCAM1, ANGPT1*). (*B*) Network 2 consists of 23 downregulated genes (*RGS4, GABRA1, GFRA2, CPLX1, KCNK9, RGS7, ARHGDIG, GABRG2, STMN2, L1CAM, SYT7, SYT5, GABRA4, KCNJ6, STX1B, GABRA5, SNAP25, PTPRN, SYT4, DUSP6, SYN1, PTPN5, PTPRN2*). (*C*) Network 3 consists of 13 downregulated genes (*IL12RB2, PRKCB, WIPF3, NRN1, ENC1, SATB1, PHACTR1, ELAVL4, FABP3, AACS, LARGE, SPTBN2, YWHAG*). Solid lines indicate direct interactions and dashed lines indicate indirect interactions. Downregulated molecules are shown in green and upregulated ones are shown in red. Encoded molecules were placed in an appropriate subcellular compartment based on IPA, if known. We added PCSK2 into Network 1, insulin, PCSK1, and PCSK2 into Network 2, and PCSK1 and PCSK2 into Network 3. PCSK1 and PCKS2 are known to be localized in secretary granules in the cytoplasm, but some amount of these proteins may be secreted into the extracellular space.

Altered Expression of DM-Related Genes in Human and Mouse AD Hippocampus

A comparison of the altered gene expression profiles in human and mouse AD brains revealed that expression of genes relevant to noninsulin-dependent diabetes and obesity was significantly altered in the presence of AD pathology, as was that of genes relevant to neuronal function or brain dysfunction (Tables 3 and 5). IPA revealed that some of the genes dysregulated in both humans and mice are regulated by insulin signaling (Figs 3 and 4*B*). *Pcsk1*, encoding proprotein convertase subtilisin/kexin type 1, which is essential for proinsulin processing together with PCSK2 (Seidah et al. 1999), was placed upstream of insulin in the mouse network along with *Ide*, encoding insulin-degrading enzyme, the expression of which was significantly increased in the hippocampus.

We then examined expression of PCSK1 protein in mouse brain by laser scanning immunofluorescence microscopy (Fig. 5). In 15-month-old male non-Tg brains, we detected PCSK1 expression in most neurons in the cerebral cortex and hippocampus (Fig. 5*A*,*B*). In non-Tg hippocampus, PCSK1 expression is prominent in CA3 and CA2 subregions and to a lesser extent in CA1 and the dentate gyrus (DG) (Fig. 5*C*). We found that expression level of PCSK1 was significantly diminished in 3xTg-AD-H brains, including in the cerebral cortex (Fig. 5*A*) and hippocampus (Fig. 5*B*,*C*), as confirmed by microarray data.

Because *PCSK1* was the second-most significantly decreased gene in human AD brains, we reconsidered the relationships among the genes in the 3 human networks and found that *PCSK2*, expression of which was also decreased in

Table 4
Altered expression of marker genes for various brain cell types in 3xTg-AD hippocampus

Cell type	Gene symbol	Relative expression (% non-Tg)	
		3xTg-AD-h	3xTg-AD-H
Astrocytes	*Gfap*	110.99	118.48
	S100b	96.74	98.40
	Aqp4	90.51	95.28
	Mean	99.41	104.05
	SD	10.50	12.59
Oligodendrocytes	*Mbp*	100.87	99.36
	Sox10	105.74	91.73
	Mog	93.31	99.61
	Mag	104.80	111.46
	mean	101.18	100.54
	SD	5.66	8.15
Microglia	*Cd68*	107.96	105.79
	Aif1	96.85	95.73
	Lgals3	82.67	92.88
	Emr1	114.35	101.75
	mean	100.46	99.04
	SD	13.89	5.82
Neurons	*Rbfox3*	104.23	100.62
	Eno2	104.26	102.52
	Chga	100.56	107.48
	Syp	100.57	99.01
	Nefh	106.52	97.41
	Nefl	102.08	100.09
	Nefm	99.64	98.33
	Snap25	99.61	98.72
	Tubb2b	104.12	104.93
	Tubb2a	103.14	106.69
	Tubb2b	100.77	105.11
	Tubb5	107.12	104.99
	Tubb4	100.68	107.81
	Tubb6	99.67	99.55
	Tubb1	101.90	100.76
	Tubb2c	93.66	92.52
	Tubb3	96.19	84.98
	mean	101.45	100.68
	SD	3.4	5.76

AD hippocampus (−1.502, $P = 0.0288$, 2-tailed *t*-test), could be placed upstream of those networks together with *PCSK1* and insulin (Fig. 3). Human Networks 1 and 3 and Mouse Network 1 are likely to represent the major insulin signaling network, in which PCSK1 and PCSK2 are essential for insulin production (Figs 3*A*,*C* and 4*B*). We then verified the human microarray data by real-time quantitative RT-PCR analyses (primers shown in see Supplementary Table S1) of 10 genes showing significant alterations as well as *PCSK2* and *PCSK5–7* in the hippocampus (see Supplementary Table S8). The relative expression level of each gene was highly correlated with the data obtained by microarray analyses (see Supplementary Fig. 2). Among the 5 *PCSK* members identified, only the expression levels of *PCSK1* and *PCSK2* were significantly decreased in AD hippocampus (see Supplementary Table S8).

To obtain data supporting the biological relevance of these changes, we examined the levels of PCSK1 and PCSK2 proteins in the hippocampus by western blot analysis. Protein levels of PCSK1 and PCSK2 were significantly decreased in AD cases compared with non-AD subjects (Fig. 6). Thus, we confirmed that the decreases in *PCSK1* and *PCSK2* mRNA levels in AD hippocampus are indeed reflected in the levels of their translation products.

Discussion

Microarray analyses of postmortem AD brains have revealed altered expression of neurological and immunological genes, genes encoding inflammatory molecules and genes encoding metabolic enzymes (Colangelo et al. 2002; Brooks et al. 2007; Parachikova et al. 2007; Bossers et al. 2010; Tan et al. 2010). Bossers et al. (2010) reported the results of a systematic search for global gene expression changes in the prefrontal cortex during the course of AD using Braak staging. They identified a number of genes involved in the processing of amyloid precursor protein and amyloid beta (*PSEN2*, *RER1*, *ZNT3*, *PCSK1*, *SST*, *PACAP*, and *EGR1*) that were initially upregulated in Braak stages I–III, but were significantly downregulated in the late Braak stages V–VI. Moreover, Tan et al. (2010) reported a significantly altered AD transcriptome in the temporal cortices of AD patients, indicative of synaptic dysfunction, perturbed neurotransmission and activation of neuroinflammation. Their lists of significantly altered AD genes contained most of the genes constituting the 3 networks shown in Figure 3 (14 of 20 genes in Network 1; 14 of 20 genes in Network 2; 4 of 13 genes in Network 3), confirming that there are common alterations of gene expression in AD brains from 2 independent cohorts (the Oxford Project to Investigate Memory and Ageing and the Hisayama study). Our study and the studies of Bossers et al. (2010) and Tan et al. (2010) all showed that expression of the *PCSK1* gene is reproducibly and most significantly downregulated in the late stages of disease in AD brains. Moreover, our data showed that the extent of *PCSK1* downregulation was most significant in the hippocampi of AD brains, with downregulation occurring to a lesser extent in the temporal cortex and to a much lesser extent in the frontal cortex, in accordance with the pathological severity.

AD Pathology May Alter Insulin Signaling

Several epidemiologic cohort studies, including the Hisayama study, have shown that individuals with DM or insulin resistance exhibit an increased risk of developing AD compared with nondiabetic individuals (Kuusisto et al. 1997; Matsuzaki et al. 2010; Schrijvers et al. 2010). Supporting these epidemiological data, induction of type 1 or type 2 DM in mouse models of AD has been reported to accelerate AD neuropathology and memory dysfunction (Jolivalt et al. 2010; Takeda et al. 2010). Conversely, mouse models of AD are likely to be more susceptible to obesity or insulin resistance (Kohjima et al. 2010). Moreover, it has been shown that insulin is produced in neuronal cells derived from the hippocampus and olfactory bulb in adult rat brain and in isolated neuronal stem cells (Kuwabara et al. 2011), suggesting that insulin produced in neurons may play important roles in the brain.

The expression levels of insulin and insulin-like growth factors I and II are known to be markedly reduced in AD brains together with decreased expression of their receptors, suggesting that AD may be a neuroendocrine disorder, namely, type 3 diabetes (Steen et al. 2005). It has also been shown that insulin prevents the loss of surface insulin receptors, oxidative stress, and synaptic spine loss in cultured mature hippocampal neurons caused by Aβ-derived diffusible ligands (De Felice et al. 2009). Moreover, administration of intranasal insulin has been reported to stabilize or improve cognition, function, and cerebral glucose metabolism in adults with mild cognitive impairment or AD (Craft et al. 2012). Taken together, our results strongly suggest that AD pathology alters insulin signaling in the brain.

In 3xTg-AD mice, insulin signaling in the hippocampus is likely to be significantly diminished based on the decreased

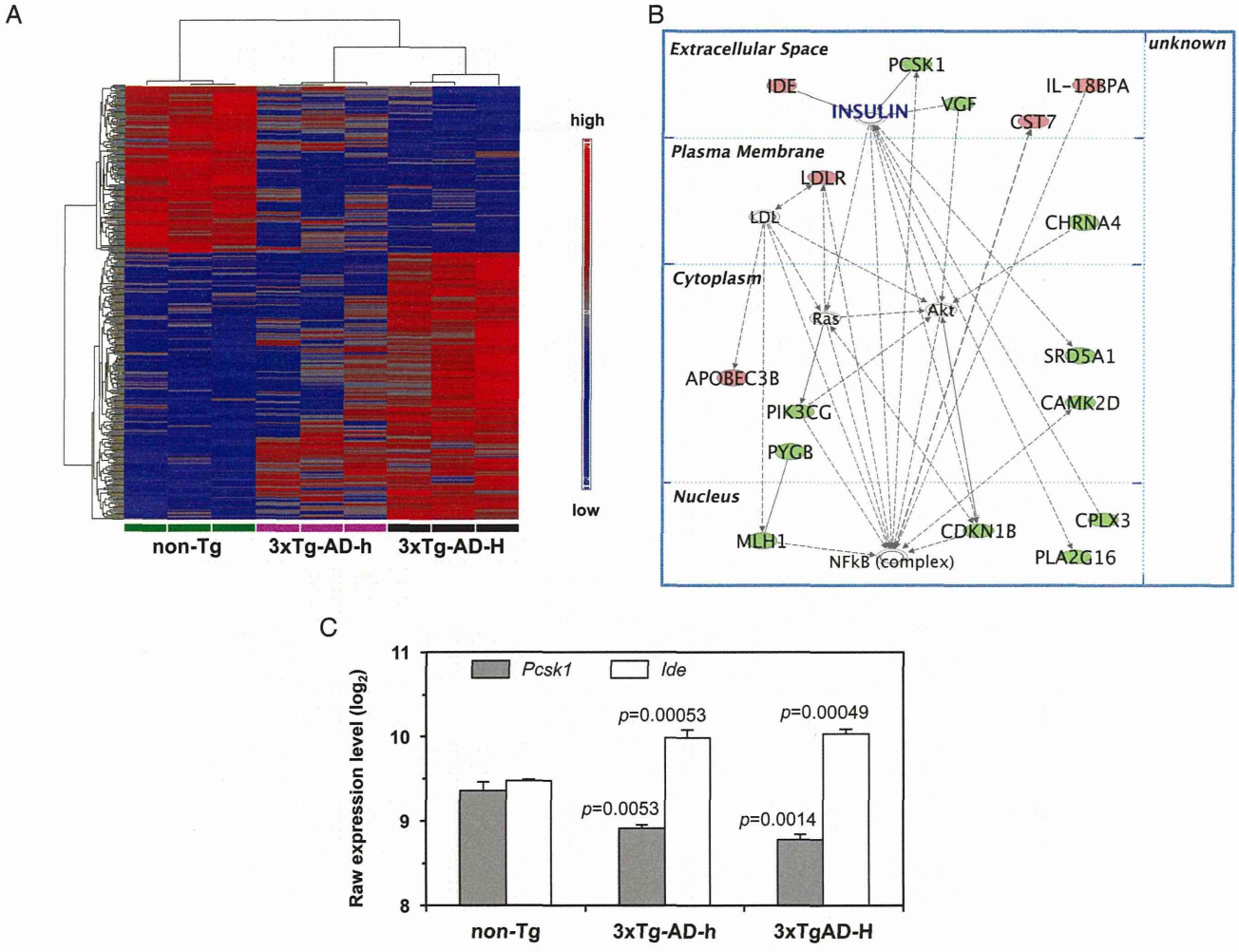

Figure 4. Results of microarray analysis of the 3xTg-AD mice. (*A*) Cluster heat map of the 406 transcript clusters based on individual expression data in the hippocampi of non-Tg (green), 3x-Tg-AD-h (magenta), and 3x-Tg-AD-H (black) mice ($N = 3$ for each group). Hierarchical and partitioning clustering of the 406 transcript clusters was performed among the 3 groups. In the heat map, blue represents a lower expression level and red indicates a higher expression level. (*B*) The top network of genes whose expression was significantly altered in the hippocampus of 3xTg-AD-H mice. Among the top 406 transcription clusters shown in Supplementary Table S7, only 120 genes were eligible for generating networks excluding microRNA–mRNA interactions; the most relevant network includes 11 downregulated genes (*Srd5a1*, *Mlh1*, *Cdkn1b*, *Pcsk1*, *Camk2d*, *Cplx3*, *Vgf*, *Chrna4*, *Pygb*, *Pik3cg*, *Pla2g16*), and 5 upregulated genes (*Cst7*, *Ide*, *Apobec3b*, *Ldlr*, *Il18bp*). Solid lines indicate direct interactions and dashed lines indicate indirect interactions. Downregulated molecules are shown in green and upregulated ones are shown in red. (*C*) Comparison of the raw expression levels for *Pcsk1* and *Ide* genes whose expression was significantly altered in the 3xTg-AD hippocampus. One-way ANOVA was performed with the list of 406 transcript clusters in hippocampus, and a *P*-value for the comparison with non-TG was determined using Fisher's Least Significant Difference method. Log_2 transformed mean values with SEMs of the raw expression levels for each gene are shown in the bar graph.

expression of downstream genes such as *Srd5a1* (Lubik et al. 2011), *Cdkn1b* (Bhatt et al. 2005) and *Pla2g16* (Duncan et al. 2008). This downregulation may be caused by a reduction in the insulin level owing to decreased expression of *Pcsk1*, and may also be due to increased expression of *Ide*, which degrades insulin and/or Aβ peptides in a competitive fashion (Farris et al. 2003). Moreover, genes involved in insulin secretion, such as *Vgf* (Watson et al. 2005) and *Cplx3* (Reim et al. 2005), were also found to be downregulated in 3xTg-AD mice in the present study (Fig. 4*B*), suggesting that AD pathology diminishes the production and secretion of insulin in brain.

In the present study, we observed significantly decreased expression of both *PCSK1* and *PCSK2* in human AD brains, which may result in a severe reduction in insulin level in AD brains. It has been shown that proinflammatory cytokines alter the expression of genes involved in insulin signaling through activation of NF-κB. For example, IFNG protein and

Table 5
List of genes significantly enriched in genetic disorders among those whose expression was significantly altered in the hippocampi of homozygous 3xTg-AD mice

Diseases and disorders	*P*-value*	Genes**
Bipolar disorder	4.64E-05	*Abca6*, *Adamts3*, *Akr1e2*, *Ca7*, *Camk2d*, *Chrna4*, *Cit*, *Cntnap5*, *Dpp10*, *Ide*, *Kcns1*, *Nme6*, *Oprd1*, *Osbpl10*, *Plxnd1*, *Ptprt*, *Rcn1*, *Slc1a1*, *Uqcc*, *Vgf*
Noninsulin-dependent diabetes mellitus	1.41E-02	*Adamts3*, *Akr1e2*, *Bfsp2*, *Ca7*, *Chrna4*, *Cntnap5*, *Glra3*, *Hpcal1*, *Ide*, *Ldlr*, *Pcsk1*, *Ptprt*, *Rai14*, *St3gal1*, *Stac*, *Tdp1*, *Unc13c*
Coronary artery disease	8.39E-03	*Adamts2*, *Adamts3*, *C9orf68*, *Camk2d*, *Cntnap5*, *Hpcal1*, *Itga8*, *Kiaa1467*, *Ldlr*, *Mamdc2*, *Pamr1*, *Ptprt*, *Pygb*, *Slc1a1*, *St3gal1*, *Tdp1*
Alzheimer's disease	1.41E-02	*Camk2d*, *Chrna4*, *Cit*, *Cntnap5*, *Fis1*, *Glt8d2*, *Ide*, *Ldlr*, *Osbpl10*, *Pamr1*, *Ptprt*, *Slc6a7*, *St3gal1*
Parkinson's disease	3.13E-02	*Ca7*, *Camk2d*, *Chrna4*, *Cntnap5*, *Cxorf40a/Cxorf40b*, *Osbpl10*, *Ptprt*, *Rai14*, *Unc13c*
Obesity	1.36E-02	*Ca7*, *Chrna4*, *Ldlr*, *Npbwr1*, *Pcsk1*, *Sstr1*, *Vgf*
Immediate hypersensitivity	1.58E-02	*Fcer1g*, *Ide*, *Klk10*, *Pik3cg*, *Stac*, *Syne2*

Note: Diseases and disorders in which more than 5 genes are enriched are listed.
*P-value by Fisher's exact test. **Upregulated genes are shown with underline.

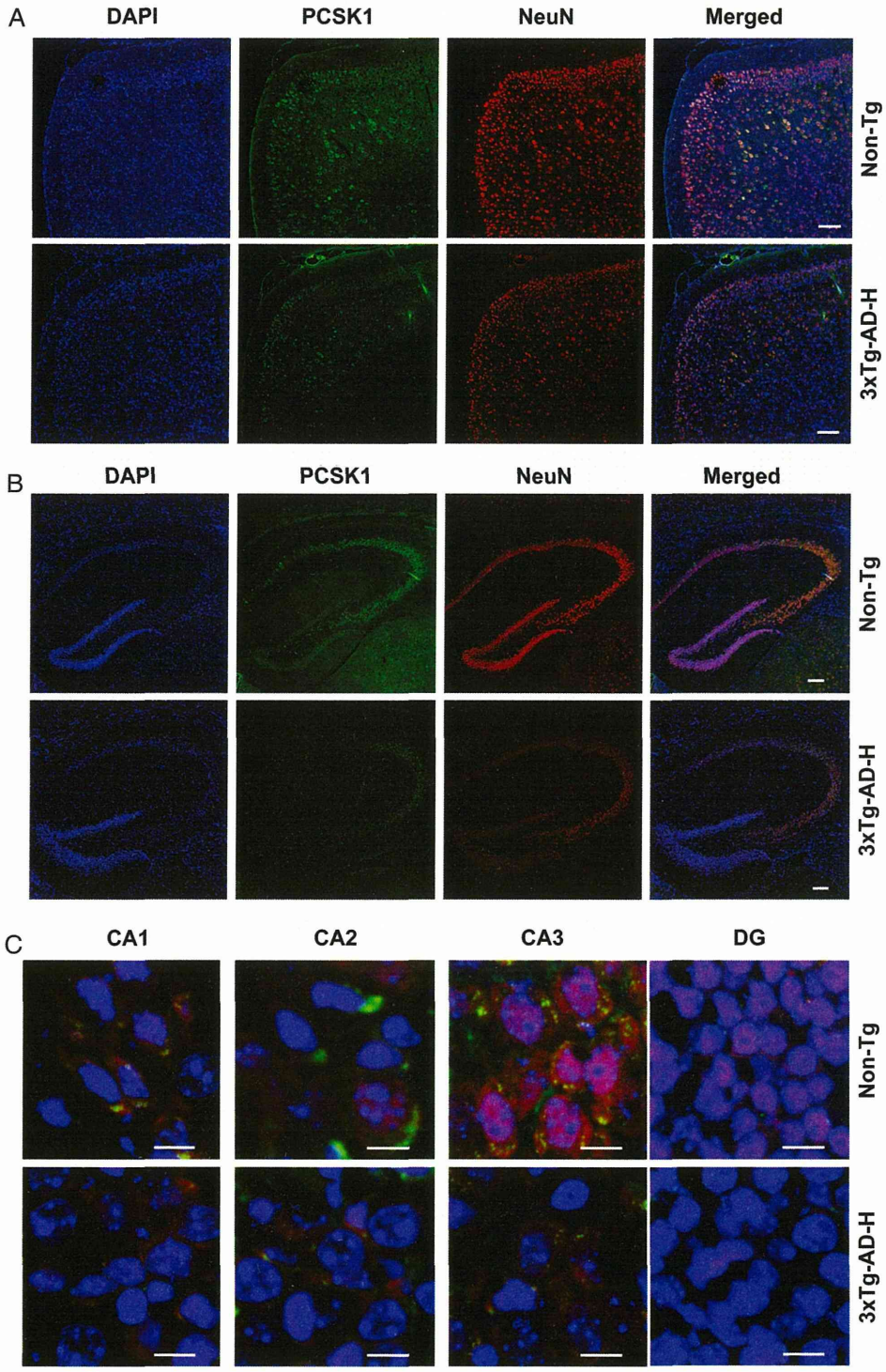

Figure 5. Evaluation of PCSK1 protein levels in mouse brain by laser scanning immunofluorescence confocal microscopy. (*A*) PCSK1 expression in the cerebral cortex. (*B*) PCSK1 expression in the hippocampus. (*C*) Magnified images of the hippocampal subregions CA1, CA2, CA3, and DG. Brain sections were prepared from 15-month-old non-Tg and 3x-Tg-AD-H male mice. Sections were reacted with anti-PCSK1 antibody (green) and an anti-NeuN antibody (red), and nuclear DNA was counterstained with DAPI (blue). Scale bars: *A*, *B*, 100 μm; *C*, 20 μm.

IL1B protein are known to decrease expression of *Pcsk1* in a process that is dependent on NF-κB in rat primary β islet cells (Cardozo et al. 2001). It has been shown that increases in the expression levels of amyloid precursor protein, presenilin-1, presenilin-2, and glycogen synthase kinase 3 (GSK3)-β in peripheral blood mononuclear cells derived from type 2 DM patients were efficiently suppressed by insulin infusion. This suppression was accompanied by significant parallel reductions in NF-κB binding activity (Dandona et al. 2011), thus suggesting that insulin may also counteract NF-κB signaling in the brain.

We also found that the gene expression profile in the brain was not significantly altered by DM or prediabetes (data not shown). Together with the observations in 3xTg-AD mice,

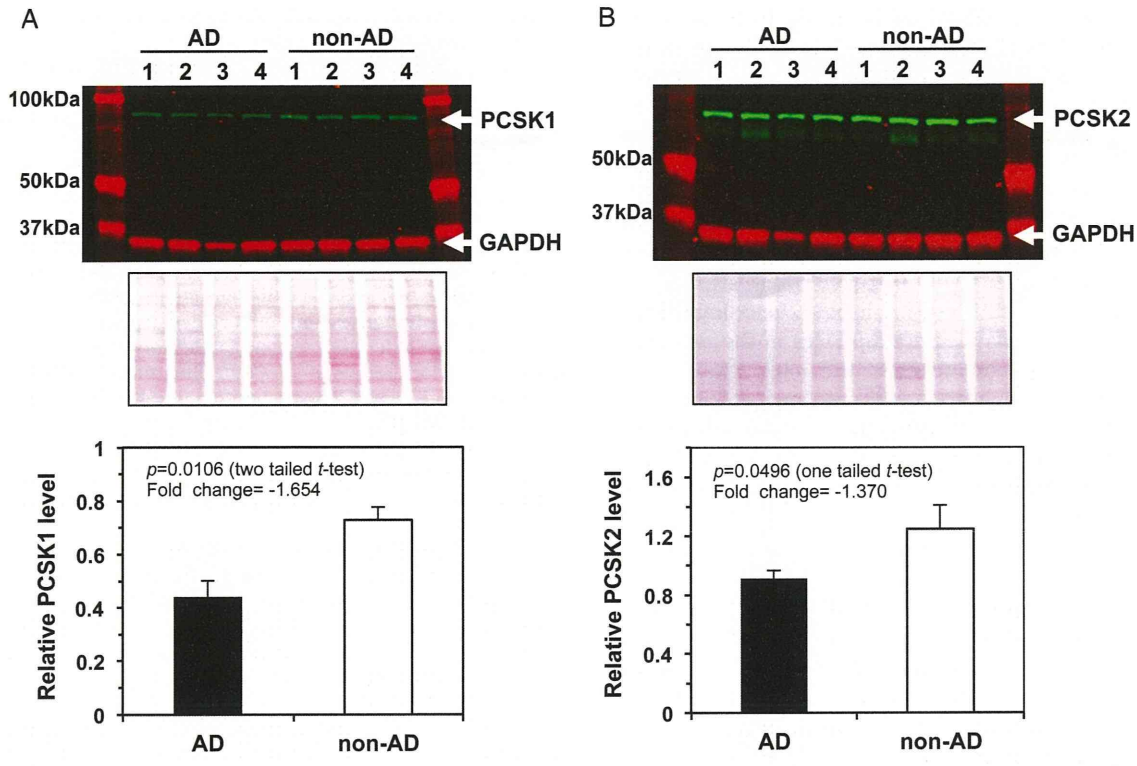

Figure 6. Evaluation of PCSK1 and PCSK2 protein levels in the hippocampal samples by western blot analysis. Hippocampal lysates (12 μg protein/lane) prepared from AD (No. 3, 4, 7, and 13 listed in see Supplementary Table S2) and non-AD brains (No. 19, 20, 21, and 28 listed in see Supplementary Table S2) were run on 10% SDS-PAGE gels and subjected to western blot analysis for PCSK1 (*A*), PCSK2 (*B*), and GAPDH proteins (top panels). Ponceau S staining (middle panels) was conducted to confirm the equal loading of samples and normalization. The relative intensities of bands were quantified using an Odyssey infrared imaging system, normalized to the intensity of Ponceau S staining, and are shown in bar graphs (bottom panels). *P*-values from an unpaired *t*-test are shown.

this finding strongly suggests that the primary AD pathology itself diminishes insulin signaling in the brain, and as such, that AD brains are more vulnerable to various pathological insults caused by metabolic impairment or inflammatory responses. Peripheral insulin resistance or DM further exacerbates AD pathology, and is thus a strong risk factor for the progression of AD. It has been reported that gastric bypass surgery for morbidly obese patients with type 2 DM significantly suppresses the increase in expression levels of AD-related genes such as amyloid precursor protein, presenilin-2, and GSK3-β in mononuclear cells, in parallel with marked weight loss and improved insulin resistance (Ghanim et al. 2012). Therefore, it is relevant that cognitive function has been shown to improve with weight loss following bariatric surgery (Gunstad et al. 2011).

Recently, it was shown that insulin-induced hypoglycemic and streptozotocin-induced diabetic rats exhibit significantly decreased expression of *GABRA1* with reduced cortical GABA binding (Antony et al. 2010; Sherin et al. 2010, 2012), indicating that Network 2 shown in Figure 3*B* also represents the effects of insulin signaling impairment owing to the decreased expression of PCSK1 and PCSK2. Moreover, silencing of the *CPLX1* gene, which is also part of Network 2 and which was also downregulated in AD brains (Fig. 3*B*), has been reported to cause strong impairment of insulin secretion in response to glucose (Abderrahmani et al. 2004). Thus, decreased expression of *CPLX1* may contribute to the insulin signaling impairment and neuronal dysfunction in AD brains.

The HGF–MET Axis May Be Involved in Insulin Signaling in Brain

Expression of *MET*, encoding a receptor for hepatocyte growth factor (HGF), was most significantly decreased in AD brains (Fig. 2*A*, see Supplementary Table S6). Expression of *MET* has been shown to be upregulated by VEGF and HGF (Gerritsen et al. 2003), and we also found that the expression level of *VEGF* is significantly decreased in AD brains, suggesting that the downregulation of *MET* gene in AD brains is likely to reflect reduced expression of VEGF, which is upregulated by insulin (Miele et al. 2000). Recently, Fafalios et al. (2011) reported that MET is essential for an optimal hepatic insulin response by directly engaging the insulin receptor (INSR) to form a MET–INSR hybrid complex culminating in a robust signal output. They also found that the HGF–MET system restores insulin responsiveness in a mouse model of insulin refractoriness. Because it has been established that insulin, HGF (Sharma 2010) and VEGF (Góra-Kupilas and Jośko 2005) have neuroprotective functions, the altered gene expression profiles in AD brains strongly suggest that a decline in the neuroprotective pathways regulated by these molecules at least partly underlies the neurodegeneration in AD brains.

Altered Expression of Transcription Factors in AD Brains

In the human AD brains, several genes encoding transcription factors were significantly downregulated (see Supplementary